11-2015

New transitions and feeding of the $J^{\pi}=(8^{+})$ isomer in ^{186}Re

David A. Matters

N. Fotiandes

J. Carroll

C. J. Chiara

John W. McClory
Air Force Institute of Technology

See next page for additional authors

Recommended Citation

Matters, D. A., et al. (2015). New transitions and feeding of the Jπ=(8+) isomer in Re186. Physical Review C (Nuclear Physics), 92(5), 54304. https://doi.org/10.1103/PhysRevC.92.054304

New transitions and feeding of the J^{π}=(8^{+}) isomer in ^{186}Re

D. A. Matters, N. Fotiades, J. J. Carroll, C. J. Chiara, J. W. McClory, T. Kawano, R. O. Nelson, and M. Devlin

Phys. Rev. C **92**, 054304 — Published 9 November 2015

DOI: 10.1103/PhysRevC.92.054304

New transitions and feeding of the $J^\pi = (8^+)$ isomer in ^{186}Re

D. A. Matters,[1,*] N. Fotiades,[2] J. J. Carroll,[3] C. J. Chiara,[4]
J. W. McClory,[1] T. Kawano,[2] R. O. Nelson,[2] and M. Devlin[2]

[1] *Air Force Institute of Technology, Wright-Patterson AFB, Ohio 45433, USA*
[2] *Los Alamos National Laboratory, Los Alamos, New Mexico 87545, USA*
[3] *U.S. Army Research Laboratory, Adelphi, Maryland 20783, USA*
[4] *Oak Ridge Associated Universities Fellowship Program, U.S. Army Research Laboratory, Adelphi, Maryland 20783, USA*

The spallation neutron source at the Los Alamos Neutron Science Center Weapons Neutron Research facility was used to populate excited states in ^{186}Re via $(n, 2n\gamma)$ reactions on an enriched ^{187}Re target. Gamma rays were detected with the the GErmanium Array for Neutron Induced Excitations spectrometer, a Compton-suppressed array of 18 HPGe detectors. Incident neutron energies were determined by the time-of-flight technique and used to obtain γ-ray excitation functions for the purpose of identifying γ rays by reaction channel. Analysis of the singles γ-ray spectrum gated on the neutron energy range $10 \leq E_n \leq 25$ MeV resulted in five transitions and one level added to the ^{186}Re level scheme. The additions include the placement of three γ rays at 266.7, 381.2, and 647.7 keV which have been identified as feeding the 2.0×10^5 yr, $J^\pi = (8^+)$ isomer and yield an improved value of 148.2(5) keV for the isomer energy. These transitions may have astrophysical implications related to the use of the Re/Os cosmochronometer.

PACS numbers: 23.20.Lv, 25.40.Fq, 27.70.+q, 28.20.-v
Keywords: NUCLEAR STRUCTURE ^{186,186m}Re; J, π, measured E_γ

I. INTRODUCTION

The Re/Os radioactive decay system is a cosmochronometer for estimating the age of astronomical objects through the measurement of the relative abundances of ^{187}Re ($T_{1/2} = 4.33 \times 10^{10}$ yr) and ^{187}Os (stable) [1]. The *s*-process nucleosynthesis of ^{187}Re and ^{187}Os includes ^{186}Re as a branch point, shown in Fig. 1. ^{186}Re in the ground state can decay with a half-life of 3.7186 d into ^{186}Os or ^{186}W or undergo neutron capture to create ^{187}Re [2, 3], but it also possesses an especially long-lived isomer ($T_{1/2} = 2.0 \times 10^5$ yr) with an excitation energy of 149(7) keV that decays 100.0% by isomeric transition to the ground state [4].

Depending on the stellar temperatures present in the *s*-process environment, the population of the ^{186}Re^m isomer may be significantly affected by the photon-induced reactions ^{186}Re$(\gamma,\gamma')^{186}$Re^m and ^{186}Re$^m(\gamma,\gamma')^{186}$Re (photoexcitation and depletion, respectively). Estimation of the cross sections for these reactions requires knowledge of the ^{186}Re level structure above the isomer, and in particular identification of intermediate states (IS) present in pathways from the ground state to the isomer and vice versa. For IS excitation energies below 1 MeV, temperatures on the order of 10^8 K can result in thermal coupling between the isomer and ground states with the potential to increase the production of the ^{186}Re^m isomer [5]. This would lead to a temperature-dependent effective half-life for ^{186}Re, which could be determined using the methodology outlined in Refs. [5–8] for ^{180}Ta and ^{176}Lu. A temperature-dependent effective half-life for ^{186}Re would affect creation of ^{187}Re and represents a potential source of error in the Re/Os chronometer.

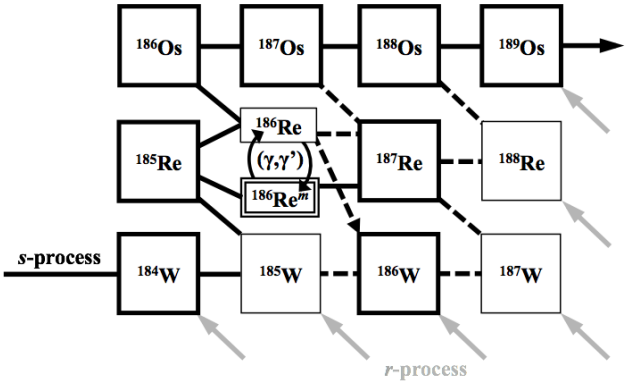

Figure 1. *s*- and *r*-processes, identified by black and gray arrows, involved in the production of ^{187}Re and ^{187}Os. Long-lived nuclides are identified with bold boxes, with the dashed lines indicating weaker secondary processes. The outline around the isomer ^{186}Re^m and the associated (γ,γ') pathways highlight the fact that their effects are not fully understood.

Based on an analysis of cross sections for neutron capture and the photodisintegration reaction ^{187}Re$(\gamma,n)^{186}$Re, Käppeler *et al.* concluded that the *s*-process contribution to ^{187}Re due to the branching at ^{186}Re was insignificant. Other than in the case of the population of the isomer via the ^{187}Re$(\gamma,n)^{186}$Re^m reaction cited in Ref. [9], the isomer's possible role in the *s*-process branching was not discussed.

Hayakawa *et al.* were the first to propose an alternate *s*-process pathway that involved the ^{186}Re^m isomer. The

* david.matters@afit.edu

group concluded that the isomer's contribution to the creation of ^{187}Re was $0.56\% \pm 0.35\%$ and is therefore an insignificant source of error in the Re/Os chronometer [10]. However, this analysis assumed that transitions between the ground state and isomer in ^{186}Re via (γ, γ') reactions were negligible, based in part on the absence of known IS by which the resonant photoexcitation/depletion reactions could proceed. Knowledge of the low-lying IS involved in photon-induced reactions requires further investigation of the structure above the isomer in ^{186}Re, and is necessary to establish conclusions about the transition probabilities between the isomer and ground state in the *s*-process environment.

Using the GErmanium Array for Neutron Induced Excitations (GEANIE) detector array at the Los Alamos Neutron Science Center (LANSCE) Weapons Neutron Research (WNR) facility, γ-ray spectra obtained from neutron-induced reactions were used to identify new γ-ray transitions in ^{186}Re and to verify transitions and levels already described in the existing literature [4, 11–16]. The primary neutron-induced reaction studied was $^{187}\mathrm{Re}(n, 2n\gamma)^{186}\mathrm{Re}$ from irradiating an enriched ^{187}Re target. Neutron energies were measured using the time-of-flight technique, and excitation functions for observed γ-ray transitions were generated and compared to those modeled using the reaction codes CoH 3.4 [17] and Talys 1.6 [18] for the purpose of placing transitions in the ^{186}Re level scheme.

II. EXPERIMENT

The LANSCE accelerator is a proton linac capable of producing beams of postively- and negatively-charged hydrogen ions with energies up to 800 MeV. For experiments at the WNR facility, spallation neutrons with energies ranging from 100 keV to 600 MeV are produced by directing pulses of H^- ions with an average current of 0.5 to 4 μA at a ^{nat}W target [19].

The GEANIE target is located 20.34 m from the spallation source along the 60° right flight path. The beam has a macropulse repetition rate of 40 or 100 Hz, with each 625-μs macropulse further divided into numerous sub-nanosecond micropulses spaced 1.8 μs apart. The pulsed nature of the beam provides the ability to measure neutron energies using the time-of-flight method, and the detection system is capable of resolving neutron energies from 0.6 to ∼200 MeV. Neutron flux at the target is measured with a fission chamber positioned at the terminus of the neutron beam tube, 18.48 m from the spallation target. The fission chamber consists of an ionization chamber that incorporates stainless steel foils coated with ^{235}U and ^{238}U, so that the known fission cross sections of these isotopes can be used to calculate the neutron flux from the counts of fission events in the ionization chamber [20]. In the $10 \leq E_n \leq 25$ MeV neutron energy range of interest for the $(n, 2n\gamma)$ reaction, the neutron fluence for the run was determined to range from $1.3 \times 10^8 - 5.0 \times 10^8$ neutrons/MeV, decreasing with increasing neutron energy. A representative profile of the fluence versus neutron energy for the GEANIE flight path can be found in Ref. [21]. The size of the neutron beam arriving at the target was trimmed to a diameter of 1.27 cm using an iron collimator, prior to the beam transiting the fission chamber. More detailed information about the LANSCE facility and the GEANIE spectrometer is available in Refs. [19, 21–23].

For this experiment, the GEANIE detector array was configured with eight planar and ten coaxial high-purity germanium (HPGe) detectors to optimize resolution and efficiency up to γ-ray energies of 4.0 MeV. Each detector was Compton suppressed using a bismuth germanate (BGO) shield. Of the 18 installed detectors, seven of each type provided usable data for offline analysis. Gamma rays were produced via neutron bombardment of a 987.1-mg target consisting of vacuum-pressed rhenium metal powder enriched to 99.52% ^{187}Re. The 1.0-mm-thick ^{187}Re target was encapsulated in a disk-shaped polycarbonate target holder. The end faces of the disk were oriented normal to the incident neutron beam. The enriched rhenium target was irradiated for 12 days at a pulse repetition rate of 40 Hz and an additional five days at 100 Hz. Energy and efficiency calibrations of the spectrometer were performed using standard ^{133}Ba and ^{152}Eu calibration sources.

III. ANALYSIS AND RESULTS

The data output by the TDCs and ADCs connected to the HPGe detectors in the GEANIE array were processed online into E_γ versus neutron time-of-flight (TOF) matrices using software based on the Midas data acquisition package [24]. The matrices, which were generated for each HPGe detector and the fission chamber, were used to produce singles γ-ray spectra gated on specified neutron-energy ranges. A neutron-energy range of $10 \leq E_n \leq 25$ MeV was used to select the γ rays that originated primarily from $(n, 2n)$ reactions on the ^{187}Re target, as shown in the spectrum of Fig. 2. Singles γ-ray spectra were fitted using the gf3 program from the RadWare software distribution [25].

For each peak identified in the singles spectrum, the matrices were gated successively on 1-MeV-wide neutron-energy bins over the energy range $1.0 \leq E_n \leq 100$ MeV, and peaks were re-fitted to produce γ-ray yield as a function of incident neutron energy. The yield functions were divided by neutron flux to produce excitation functions for each distinct γ-ray energy. For γ rays originating from the $^{187}\mathrm{Re}(n, 2n\gamma)^{186}\mathrm{Re}$ channel, the excitation functions rise quickly following the ^{187}Re neutron separation energy of $S_n = 7.3568$ MeV [26] to peak at neutron energies between 10 and 20 MeV [27], then decrease rapidly as the $(n, 3n\gamma)$ reaction becomes energetically favorable. The distinctive shape of the $(n, 2n\gamma)$ excitation functions distinguishes the ^{186}Re γ rays from those produced in the

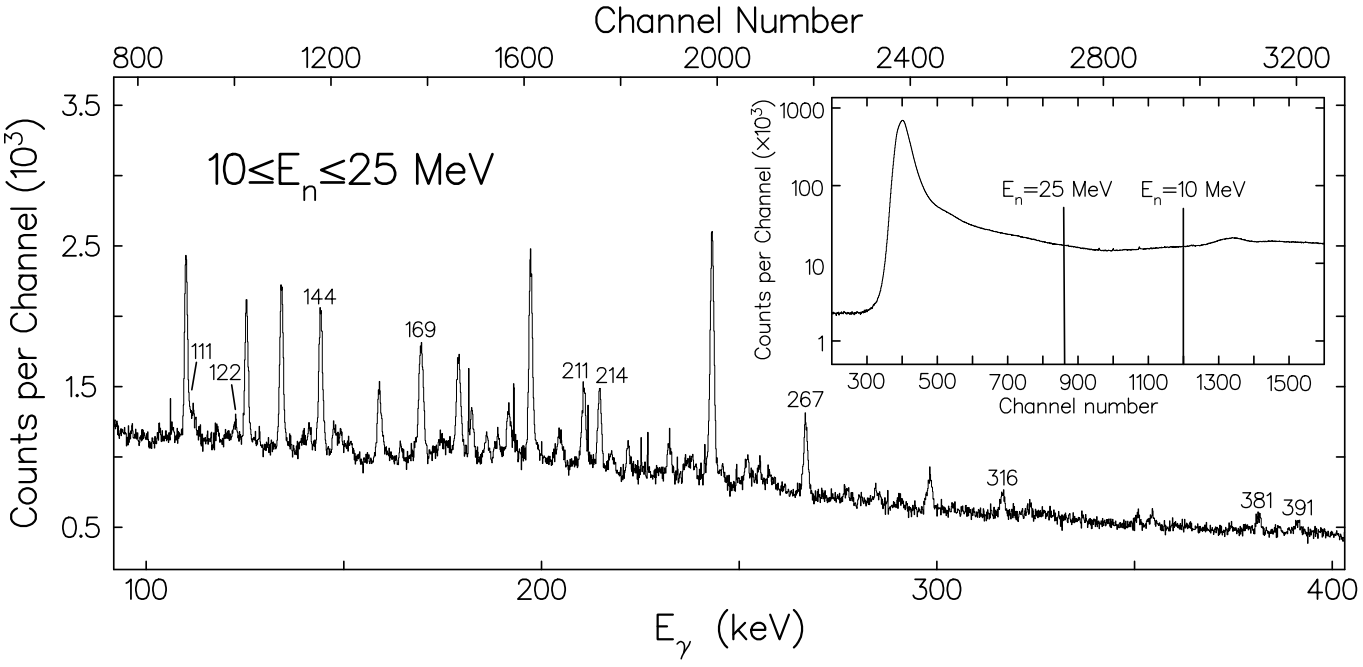

Figure 2. Summed γ-ray spectrum from the planar HPGe detectors, gated on $10 \leq E_n \leq 25$ MeV. Prominent peaks due to ^{186}Re are labeled by energy in keV, up to 400 keV. Unlabeled peaks were identified as γ rays from reactions other than $^{187}\mathrm{Re}(n, 2n\gamma)^{186}\mathrm{Re}$. The inset shows the projection of the E_γ-vs.-neutron-TOF matrix on the TOF axis and the channel locations corresponding to the neutron energy cuts of 10 and 25 MeV.

$(n, n'\gamma)$ and $(n, 3n\gamma)$ reaction channels, which result in excitation functions that rise and peak at neutron energies approximately 7.5 MeV lower or higher, respectively, than that of the $(n, 2n\gamma)$ channel.

Gamma rays originating from the $^{187}\mathrm{Re}(n, pn\gamma)^{186}\mathrm{W}$ channel also have excitation functions with a positive slope in the 10–20 MeV neutron-energy range, similar to those from the $(n, 2n\gamma)$ channel. The $(n, pn\gamma)$ excitation functions, however, show a distinctly different behavior at neutron energies above 20 MeV, where they decay much more slowly than do the $(n, 2n\gamma)$ excitation functions. To support the assignment of γ rays to ^{186}Re instead of ^{186}W in this analysis, the areas of the γ-ray peaks in the gated ($10 \leq E_n \leq 25$ MeV) projection spectrum were compared to those from the most intense γ rays in ^{186}W, the 122.64-keV $2^+ \rightarrow 0^+$ and 273.93-keV $4^+ \rightarrow 2^+$ transitions [4]. The spectrum shown in Fig. 2 reveals the presence of a 122-keV peak, which is due partly to the 122.525-keV γ ray from the $(4)^- \rightarrow (3)^-$ transition in ^{186}Re, while no peak at 273.93 keV is evident. No other γ rays from ^{186}W were identifiable in the gated spectrum. This observation is supported by the fact that the ENDF/B-VII.1 total cross section at $E_n = 15$ MeV for the $^{187}\mathrm{Re}(n, pn)^{186}\mathrm{W}$ reaction is over two orders of magnitude smaller than that of the $^{187}\mathrm{Re}(n, 2n)^{186}\mathrm{Re}$ reaction [28]. Unknown γ rays with excitation functions that met the $(n, 2n\gamma)$ criteria discussed above were therefore attributed to ^{186}Re.

A total of 29 γ-ray peaks in the singles spectrum were attributed to ^{186}Re, including nine γ rays cataloged in Table I that are not included in the evaluated level scheme [4]. A 1969 work by Lanier *et al.* also identified 186.00(8)-, 217.91(10)-, 266.70(20)-, and 354.10(5)-keV γ-ray transitions in ^{186}Re, similar in energy to four of the γ rays listed in Table I, which were not placed in the ^{186}Re level scheme [4, 12]. These γ rays were observed in prompt γ-ray spectra from $(n_{\mathrm{thermal}}, \gamma)$ reactions on ^{185}Re, measured using a bent-crystal spectrometer during irradiation of a sample of 79.2% ^{185}Re and 20.8% ^{187}Re at Risø, Denmark [12].

Table I. Energies of γ rays attributed to ^{186}Re in this work that are not included in the evaluated level scheme [4]. Gamma rays were attributed to ^{186}Re based on an analysis of their excitation functions. Asterisks indicate γ rays observed but not placed in the level scheme in this work.

E_γ^{exp} (keV)	E_γ^{exp} (keV)	E_γ^{exp} (keV)
185.99(6)*	290.51(13)*	647.7(2)
217.62(10)*	354.28(9)*	1007.5(3)
266.69(4)	381.23(7)	1101.3(3)

The shapes of the excitation functions were further used to estimate the spin of the initial level of each observed transition. Transitions originating from low-spin states have excitation functions that rise sharply after the threshold energy of the $(n, 2n)$ reaction to peak at neutron energies near 13 MeV, while those originating from high-spin states rise more gradually and peak at neutron energies between 15 and 20 MeV. This effect is

evident in Fig. 3, in which excitation functions for known 111.7- and 188.8-keV γ-ray transitions in ^{186}Re are compared with that of the 266.7-keV transition assessed to originate from a high-spin state.

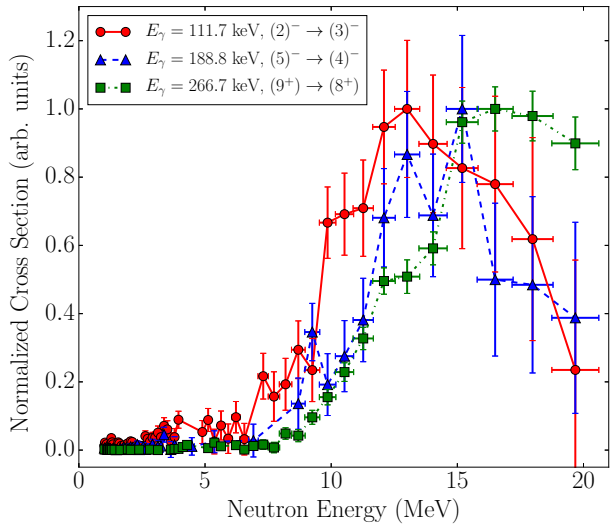

Figure 3. (Color online) Experimental excitation functions for the 111.7-, 188.8-, and 266.7-keV γ-ray transitions in the ^{187}Re$(n, 2n\gamma)^{186}$Re reaction channel, normalized for the purpose of comparing their shapes. Excitation functions for transitions that originate from higher-spin states show a slower rise after the reaction threshold energy than do those originating from low-spin states. The excitation function for the 266.7-keV transition is included in the plot according to its assignment in this work as deexciting a (9^+) level to feed the (8^+) isomer.

The transitions and levels placed in the ^{186}Re level scheme in this work are listed in Table II and illustrated in the partial level scheme shown in Fig. 4. Gamma rays previously reported were placed according to their assignment in the evaluated literature [4, 11–15]. Five of the nine transitions listed in Table I were added to the level scheme based on energy differences of levels reported in Refs. [4, 16] and an analysis of their excitation functions. There was insufficient information to guide the placement of the remaining four transitions, identified with asterisks in Table I, so these were not included in the level scheme.

γ-γ coincidence matrices were also generated during offline data analysis, but the statistics from the γ-ray peaks produced with the neutron-energy gates of $10 \leq E_n \leq 25$ MeV applied were insufficient to assist in developing the ^{186}Re level scheme. The lack of useful coincidence data prevented the elimination of background contributions from other reaction channels in the examination of transitions of interest in ^{186}Re. Because the majority of observed γ-ray transitions showed contributions from reactions other than $(n, 2n\gamma)$ in their excitation functions, γ-ray intensities for decays in ^{186}Re could not be reliably determined and thus are not reported.

The ^{186}Re level scheme had previously been investi-

Table II. Excitation energies, spin-parities, and transition energies for all levels and γ rays shown in Fig. 4. Excitation energies E_x and spin-parity values J^π are the literature values unless identified in bold italics to indicate values proposed in this work. Experimental γ-ray energies E_γ^{exp} were obtained by fitting the gated $10 \leq E_n \leq 25$ MeV spectrum of Fig. 2. Literature values E_x^{lit} and E_γ^{lit} for excitation and γ-ray energies are shown in the second and fifth columns for comparison and are taken from the adopted values listed in Ref. [4] unless otherwise indicated.

E_x (keV)	$E_x^{\rm lit}$ (keV)	J^π	$E_\gamma^{\rm exp}$ (keV)	$E_\gamma^{\rm lit}$ (keV)
0.0	0.0	1^-		
59.010(3)	59.010(3)	$(2)^-$		
99.361(3)	99.361(3)	$(3)^-$		
146.274(4)	146.274(4)	$(3)^-$		
148.2(5)	149(7)	(8^+)		
$\sim$ 186	$\sim$ 186	$(6)^-$		
210.699	210.699	$(2)^-$	111.74(5)	111.337(8)
			151.38(8)	151.686(5)
			210.74(6)	210.685(17)
268.798	268.798	$(4)^-$	122.45(6)	122.525(5)
			169.44(11)	169.431(8)
			210.12(10)	209.82(2)
273.627(5)	273.627(5)	$(4)^-$		
314.009	314.009	$(3)^+$	214.60(3)	214.648(8)
			255.05(6)	254.995(15)
316.463	316.463	$(1)^-$	257.45(7)	257.446(15)
			316.45(5)	316.473(20)
322.379(6)	322.379(6)	$(3)^-$		
$\sim$ 330	$\sim$ 330	$(5)^+$	144.08(2)	144.152(5)
351.202(16)	351.202(16)	$(3)^+$		
414.9(5)[a]	414.9(5)[a]	***(9$^+$)***	266.69(4)	266.70(20)[b]
420.559(7)	420.559(7)	$(4)^+$		
462.969	462.969	$(5)^-$	188.79(7)	189.313(17)
469.779	469.779	$(4)^-$	147.60(7)	147.417(6)
$\sim$ 471	$\sim$ 471	$(4)^+$	141.23(6)	141.257(5)
500.722	500.722	$(4)^+$	149.23(8)	149.520(5)
559.976	559.976	$(5)^+$	139.62(12)	139.416(7)
588.709	588.709	(4^-)	117.92(13)	118.196(4)
601.58	601.58	$(1)^+$	391.09(11)	390.91(5)
623.89	623.89	(1^-)	413.53(12)	413.21(6)
665.188	665.188	$(5)^+$	164.7(3)	164.466(8)
796.1(5)		***(10$^+$)***	381.23(7)	
			647.7(2)	
1007.5(3)	1007.4(20)[a]		1007.5(3)	
1101.3(3)	1101.9(5)[a]	$(2^-, 3^-)$	1101.3(3)	

[a] Proposed in Ref. [16]
[b] Proposed in Ref. [12]

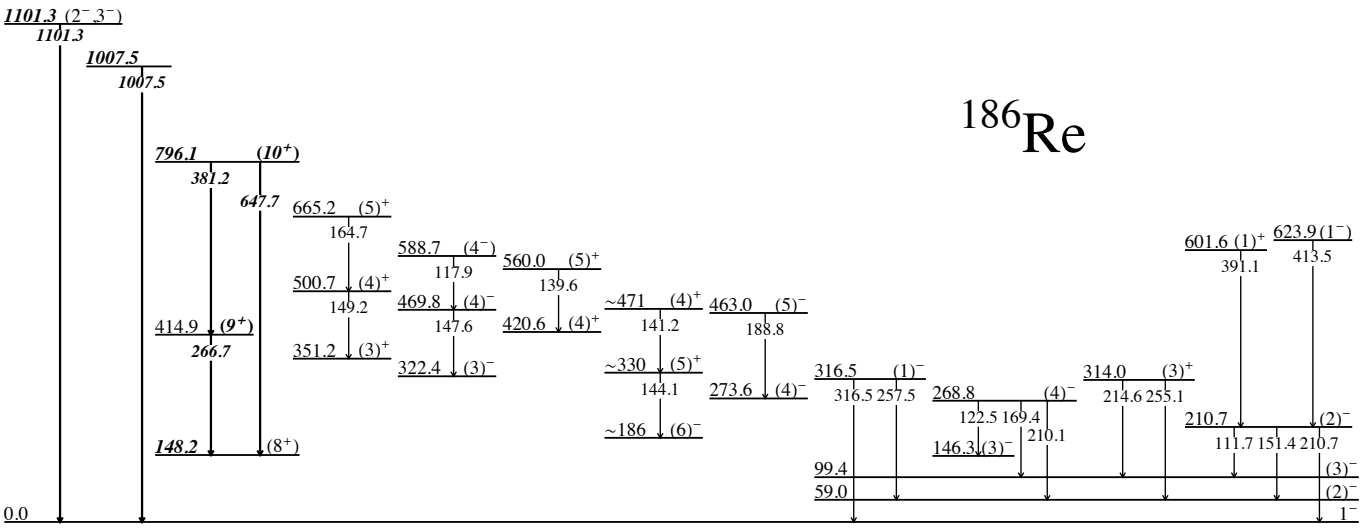

Figure 4. Partial level scheme for ^{186}Re showing the transitions observed in this work, with energies labeled in keV and tentative assignments identified with parentheses. Levels or transitions with properties in bold italics indicate proposed level energies and spin-parity assignments or transitions placed in this work. All other level energies and spin-parity assignments are those in the adopted level scheme for ^{186}Re [4].

gated primarily with information obtained from (n,γ), (d,p), and (d,t) reactions, so the low-spin ($\leq 6\hbar$) portion of the level scheme is well-developed [4]. A 2009 paper by Wheldon *et al.* described over 30 new levels in ^{186}Re populated by (p,d) reactions on ^{187}Re at proton energies of 21 MeV, including higher-spin states not yet included in the evaluated data file [4, 16]. Measurement of the deuteron energies using a magnetic spectrograph, combined with knowledge of the incident proton energy, permitted the group to calculate excitation energies and population intensities of levels in the (p,d) reaction.

Several of the states first reported by Wheldon *et al.* were observed to be populated in the $(n,2n)$ reaction described in this work. The 1007.5- and 1101.3-keV γ rays were placed based on the existence of levels at energies 1007.4(20) keV and 1101.9(5) keV reported in Ref. [16]. Of greater significance to this study was the 414.9(5)-keV level populated in the (p,d) reaction, which was identified in Ref. [16] as a higher-spin state with a possible spin-parity assignment of $J^\pi = 7^-$. In this work, the 414.9(5)-keV level was assessed as directly feeding the 149(7)-keV isomer via a 266.69(4)-keV transition, providing an improved estimate of 148.2(5) keV for the isomer energy.

The assignment of the 266.7-, 381.2-, and 647.7-keV transitions above the isomer in the level scheme of Fig. 4 is supported by similarities between ^{186}Re and the neighboring odd-odd isotope ^{184}Re. Both isotopes have long-lived isomers in the 140- to 190-keV energy range, with equivalent $(\pi 5/2[402]) + (\nu 11/2[615])$ configurations [4, 11, 29]. Evaluated nuclear data reveals a well-defined structure above the $J^\pi = 8^{(+)}$ isomer in ^{184}Re, which includes 446.0-keV, $J^\pi = (9^+)$, and 727.9-keV, $J^\pi = (10^+)$, levels feeding the 188.0-keV isomer. Expecting the level structure above the isomer in ^{186}Re to show similarities to that in ^{184}Re, the analogous levels are those at 414.9 keV and 796.1 keV. The new level in ^{186}Re at 796.1 keV deexcites by emission of 381.2- and 647.7-keV γ rays. On the basis of the similar high-spin components in the excitation functions for the 381.2- and 647.7-keV γ rays, the spin-parity assignment for the 796.1-keV level is proposed as $J^\pi = (10^+)$ in this work.

Further motivating the assignment of levels above the isomer in ^{186}Re is the output from the reaction models CoH 3.4 and Talys 1.6 for a variety of considered spin assignments for the 414.9- and 796.1-keV levels. Both CoH 3.4 and Talys 1.6 incorporate an optical model and Hauser-Feshbach statistical calculations to simulate partial γ-ray cross sections given discrete level information for the nuclei involved in the reactions of interest. Due to the presence in the spectrum of γ rays from reactions other than $(n,2n\gamma)$, experimental excitation functions included some fraction of the yield from all reaction channels that produced γ rays close to a given energy. To model this appropriately, the simulated partial cross sections from CoH 3.4 and Talys 1.6 for γ rays in the ^{187}Re$(n,2n\gamma)^{186}$Re reaction channel were added to those from similar-energy γ rays produced in $(n,n'\gamma)$ and $(n,3n\gamma)$ reactions. The experimental and simulated excitation functions were then normalized for the purpose of comparing their shapes, revealing in some cases a double peak when the partial γ-ray cross sections from different reaction channels had similar magnitudes.

In the case of the 266.7-keV γ-ray transition, the models demonstrate a poor fit to the experimental excitation function when the 414.9-keV level is assumed to have a spin less than $9\hbar$, evident in the plot shown in Fig. 5. For the 381.2-keV γ-ray transition, the models demonstrate acceptable fits to the experimental excitation function only when the 796.1-keV level is assumed to have a

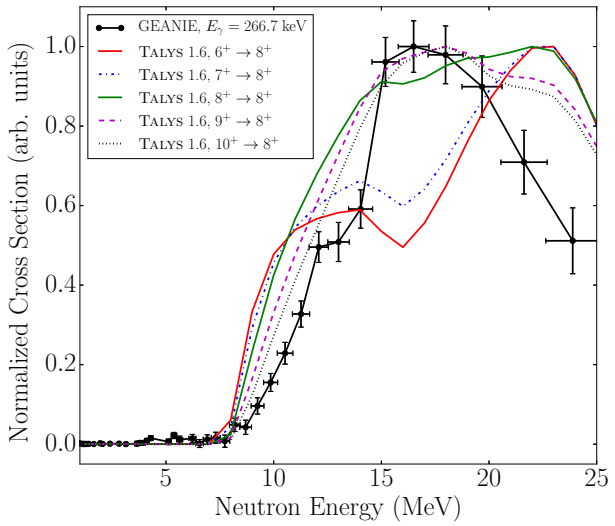

Figure 5. (Color online) Experimental and TALYS-modeled excitation functions for the 266.7-keV γ-ray transition in the ^{187}Re$(n, 2n\gamma)^{186}$Re reaction channel, normalized for the purpose of comparing their shapes. TALYS input was modified to include several spin-parity assignments for the initial level to rule out low-spin states feeding the isomer. The shapes of the $6^+ \to 8^+$, $7^+ \to 8^+$, and $8^+ \to 8^+$ excitation functions reveal contamination from the 267-keV transition in ^{185}Re produced in the $(n, 3n\gamma)$ reaction channel.

spin of $10\hbar$ or greater. Output from CoH 3.4 is similar to that produced by TALYS 1.6, and the shapes of the modeled excitation functions show only a minor parity dependence.

For each of the new transitions placed in the ^{186}Re level scheme, the experimental excitation functions were compared with those from CoH 3.4 and TALYS 1.6 for the proposed assignments in Table II and Fig. 4. Examples for the 266.7-, 381.2-, and 647.7-keV transitions are shown in Fig. 6.

The 796.1-keV level is not as strongly populated as the 414.9-keV level, so the lower-intensity 381.2- and 647.7-keV γ rays produce excitation functions with larger error bars than those of the 266.7-keV γ ray. However, both models reproduce the general shapes of the experimental excitation functions and suggest that all three γ rays originate from high-spin states as proposed in Table II and Fig. 4.

IV. CONCLUSIONS

The significant outcome of this experiment was enriching the ^{186}Re level scheme with the addition of five newly placed transitions and one new level. In particular, the structure above the 2.0×10^5 yr isomer in ^{186}Re has not been previously reported, and new γ-ray transitions observed in the ^{187}Re$(n, 2n\gamma)^{186}$Re reaction channel may be evidence of pathways by which the isomer is populated. Comparison of experimental and simulated excita-

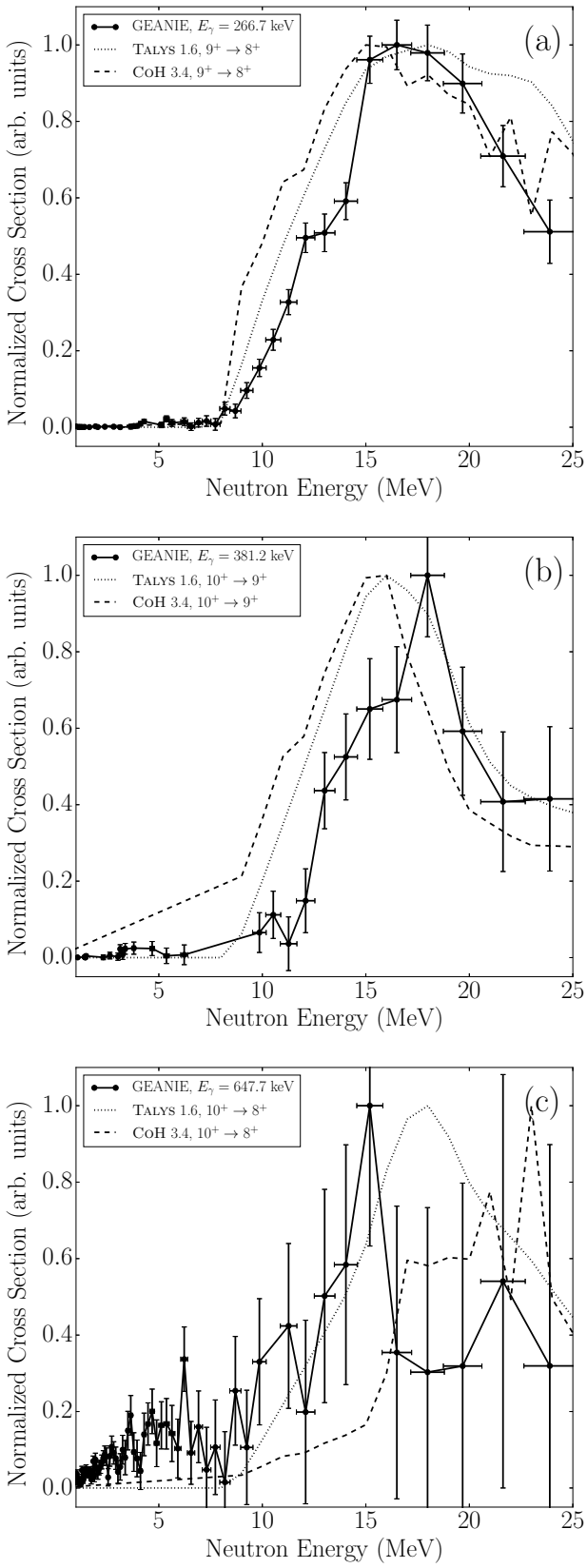

Figure 6. Excitation functions up to 25-MeV incident neutron energy for the (a) 266.7-, (b) 381.2-, and (c) 647.7-keV γ rays observed in the GEANIE data. Plots are overlaid with simulated excitation functions from CoH 3.4 and TALYS 1.6 for the assignments proposed in Table II and Fig. 4.

tion functions for the observed γ-ray transitions confirm the high-spin ($J \geq 7\hbar$) nature of certain levels populated in the $(n, 2n)$ reaction, while similarities between the neighboring odd-odd isotopes ^{184}Re and ^{186}Re motivated the assignment of levels and transitions above the isomer.

The new transitions identified in this work lead to an improved determination of the excitation energy of the ^{186}Re^m isomer with a smaller uncertainty than the reference value. The energy adopted in Ref. [4] for the 2.0×10^5 yr isomer in ^{186}Re is 149(7) keV, based solely on the work of Seegmiller *et al.* [11]. The 266.69(4)-keV γ ray attributed to ^{186}Re is proposed in this work to be a transition to the isomeric state from the 414.9(5)-keV level identified by Wheldon *et al.* [16]. This places the isomer energy at 148.2(5) keV, an order-of-magnitude improvement in uncertainty compared to the adopted value.

The observation of transitions feeding the isomer from higher-lying levels is a first step toward evaluating ^{186}Re as a branch point for stellar nucleosynthesis. Of future interest are the energies of low-lying IS in ^{186}Re which have decay branches leading towards both the isomer and the ground state. Such IS, which may deexcite via the 266.7-, 381.2-, and 647.7-keV transitions described in this work, are critical to the population or depopulation of the ^{186}Re^m isomer via (γ, γ') reactions in stellar environments. With knowledge of the astrophysically relevant IS involved in these resonant reactions, probabilities for isomer photoactivation and depletion can be estimated and the associated effects on the accuracy of the Re/Os chronometer evaluated.

V. ACKNOWLEDGMENTS

This work was supported by the U.S. Department of Energy and has benefited from use of the LANSCE accelerator facility under contract DE-AC52-06NA25396. This work was also supported by the Army Research Laboratory under Cooperative Agreement W911NF-12-2-0019. Target samples were provided by Ecopulse, Inc. Additional funding was provided by the Defense Threat Reduction Agency and the Domestic Nuclear Detection Office of the Department of Homeland Security.

[1] D. D. Clayton, Astrophys. J. **139**, 637 (1964).
[2] F. Käppeler, S. Jaag, Z. Y. Bao, and G. Reffo, Astrophys. J. **366**, 605 (1991).
[3] F. Käppeler, A. Mengoni, M. Mosconi, K. Fujii, M. Heil, C. Domingo-Pardo, and the n_TOF collaboration, J. Korean Phys. Soc. **59**, 2094 (2011).
[4] C. M. Baglin, Nucl. Data Sheets **99**, 1 (2003).
[5] D. Belic et al., Phys. Rev. Lett. **83**, 5242 (1999).
[6] J. J. Carroll, J. A. Anderson, J. W. Glesener, C. D. Eberhard, and C. B. Collins, Astrophys. J. **344**, 454 (1989).
[7] C. B. Collins et al., Phys. Rev. C **42**, R1813 (1990).
[8] D. Belic et al., Phys. Rev. C **65**, 035801 (2002).
[9] P. Mohr, S. Goriely, T. Shizuma, and T. Hayakawa, in *PoS (NIC-IX) 142* (2006), International Symposium on Nuclear Astrophysics.
[10] T. Hayakawa, T. Shizuma, T. Kajino, S. Chiba, N. Shinohara, T. Nakagawa, and T. Arima, Astrophys. J. **628**, 533 (2005).
[11] D. W. Seegmiller, M. Lindner, and R. A. Meyer, Nucl. Phys. **A185**, 94 (1972).
[12] R. G. Lanier et al., Phys. Rev. **178**, 1919 (1969).
[13] J. Glatz, Z. Phys. **265**, 335 (1973).
[14] F. Becvar, Y. Gonzatko, M. Kralik, N. D. Nhuan, T. Stadnikov, and S. A. Telezhnikov, Yad. Fiz. **37**, 1357 (1983).
[15] F. Becvar, Y. Gonzatko, M. Kralik, N. D. Nhuan, T. Stadnikov, and S. A. Telezhnikov, in *Proc. Conf. Neutron Physics, Kiev* (1980), vol. 2, p. 224.
[16] C. Wheldon et al., J. Phys. G **36**, 95 (2009).
[17] T. Kawano, P. Talou, M. B. Chadwick, and T. Watanabe, J. Nucl. Sci. Tech. **47**, 462 (2010).
[18] A. J. Koning, S. Hilaire, and M. C. Duijvestijn, in *Proceedings of the International Conference on Nuclear Data for Science and Technology*, edited by O. Bersillon, F. Gunsing, E. Bauge, R. Jacqmin, and S. Leray (EDP Sciences, 2008), pp. 211–214.
[19] P. W. Lisowski and K. F. Schoenberg, Nucl. Instrum. Methods A **562**, 910 (2006).
[20] S. A. Wender et al., Nucl. Instrum. Methods A **336**, 226 (1993).
[21] N. Fotiades et al., Phys. Rev. C **69**, 024601 (2004).
[22] P. W. Lisowski, C. D. Bowman, G. J. Russell, and S. A. Wender, Nucl. Sci. Eng. **106**, 208 (1990).
[23] J. A. Becker and R. O. Nelson, Nuclear Physics News International **7**, 11 (1997).
[24] MIDAS *home page*, URL `https://midas.triumf.ca`.
[25] D. Radford, RADWARE *home page*, Oak Ridge National Laboratory, URL `http://radware.phy.ornl.gov/main.html`.
[26] M. S. Basunia, Nucl. Data Sheets **110**, 999 (2009).
[27] N. Fotiades, R. O. Nelson, M. Devlin, and J. A. Becker, Phys. Rev. C **77**, 024306 (2008).
[28] *Evaluated Nuclear Data File (ENDF) database*, URL `https://www-nds.iaea.org/exfor/endf.htm`.
[29] C. M. Baglin, Nucl. Data Sheets **111**, 275 (2010).